European Rotorcraft Forum

APPROACHES FOR NUMERICAL ANALYSIS AND EXPERIMENTAL MONITORING OF MANUFACTURING PROCESS AND DAMAGE EVOLUTION IN CARBON/TITANIUM HYBRID STRUCTURES

S. Ghiavsand*[1], A. Airoldi[1], P. Bettini[1], G.M. Capizzi[1], and P. Bogotto[2]

[1]Dept. of Aerospace Science and Technlogy, Politecnico di Milano, Via La Masa, 34 -20156 - Milano ITALY
[2]Aerea S.p.A., Via C. Cattaneo, 24 -22078 - Turate (CO)- ITALY
*sara.ghiasvand@polimi.it

Abstract

The prediction of detailed mechanical respond in bonded Composite/Metal hybrid structure is hardly detectable due to the presents of thermal strain that depends on mismatch of Coefficient of Thermal Expansion (CTE), adhesive behavior, development of defects in adhesive layer during manufacturing or operational loads. These uncertainties could be overcome by optical fibre based monitoring systems and by a precise characterization of the manufacturing effects and damage progression on the stress-strain field. This paper presents a well-assessed monitoring technique based on strain sensors carried by optical fibers embedded in the hybrid specimen that can be used both during manufacturing process and fracture test to validate a numerical modelling approach for prediction of strain evolution. The experimental tests are conducted with two pre-damaged configurations, Balanced and Un-Balanced specimens equipped by two types of fiber coating, Naked fiber and Ormocer, to investigate the effects of thermal stress build-up on the fracture behavior. The hybrid specimens have been designed by the method that is capable of controlling thermal stress build-up. These specimens have been obtained by co-bonded process and have been suited for the Double cantilever Beam (DCB) fracture mechanic test. Validated numerical approach based on multistep explicit analyses have been used to implement the effect of thermal stress produced in the manufacturing on the simulation of fracture propagation.

1. INTRODUCTION

Structural Health Monitoring (SHM) denotes a system with the ability to detect and interpret ”changes” in the structure, in order to improve reliability and reduce life-cycle costs. The greatest challenge in designing a SHM system is to recognize what ”changes” to look for and how to identify them [1]. In this context, SHM system can be defined as several sensors that providing information to locate, evaluate and predict the damage conditions of a structure. SHM of aircraft's structures could perform real time inspections and simultaneously reduce costs, and improve the reliability and performance of these structures. The feasible SHM for an aircraft should fulfill the requirements of being reliable and profitable, in order to reduce inspection efforts and downtimes. To accomplish such objectives, previous studies have shown that Fiber Bragg Grating (FBG) sensors are suitable candidates, thanks to their intrinsic capabilities, such as high sensitivity, compact size, light weight, immunity to electromagnetic field interference, capability of working in high-temperature environment, high life durability, no limitation on the number of sensors embedment [2-3].

The focus of many works in structural health monitoring is localized in parameter monitoring such as strain, temperature or pressure. One application where such monitoring is useful is fabrication of composite materials. Indeed, this process induces stress and strains which can lead to significant problems such as in the case of development of thermal stress caused by mismatch of Coefficient of Thermal Expansions (CTE's). Although thermal residual stresses exist in many engineering compo-

nents, due to the complexity of their nature, some designers ignore them in the design process; However, the magnitude of these stresses is often significant, as in the case of metallic/composite assembly, and ignoring them at the design stage may result in a risky design. Moreover, residual stresses could be useful and improve the performance of the component under load-bearing conditions; therefore, a precise knowledge of curing conditions is required.

The sensor for such application must be able to survive the curing temperatures and be capa-ble of discriminating between multiple parameters. In 1990, Dunphy et al. [4] employed the Fiber Bragg Grating embedded into composite materi-als to monitor the vitrification during curing pro-cess. Kuang and collegues [5] improved detect-ing effect of the sensors by embedding FBG into composite materials in different layers. By using a similar techniqu, Okabe et al. [6] utilized small-diameter FBG's to study residual stress with micro damage of inner structure of the composite. Fur-thermore, FBG has been also used to monitor the epoxy curing and found the glass transition temperature with intensity changes [7-9]. The development of thermal residual stress and distortions during the curing process of composite parts have also been extensively studied [10-12]. In sev-eral other works, FBG's have been proved to be applicable to detect anomalies produced by damage evolution [13-17].

It is also worth noting that thermal stress, which are accumulated during manufacturing process, can be released by evolution of damage. The release of thermal stress by damage can cause anomalies in strain field even in unloaded condition. Therefore, a quantitative prediction of such phenomenon is of fundamental importance to design health monitoring networks which can detect sub-critical damage at the critical interfaces of hybrid structures.

The aim of this activity is investigating and characterizing delamination phenomena at the interfaces of carbon fibre reinforced composite laminates and layers of titanium alloy by experimental and numerical approach. Moreover, the results of this activity can show detectability of SHM networks for damage evolution in the interface of bonded hybrid structure. For this purpose, FBG sensorized specimen have been used for monitoring of manufacturing process and subsequently for mechanical tests. Numerical modelling with the help of cohesive zone modelling have been used to predict the residual stress in cooling phase of the manufacturing and the evolution of strains during delamination development.

2. MANUFACTURING OF HYBRID SPECIMENS WITH EMBEDDED OPTICAL FIBRES

2.1. Design of specimens and monitoring system

In this work, Interfaces between layers of hybrid specimen of Ti-6AL-4V titanium alloy and composite pre-pregs with unidirectional IM7 fibres and Hexcel 8552 epoxy matrix, have been studied. Double Cantilever Beam (DCB) test, is typically used to evaluate the mode I fracture toughness of interfaces. To study the thermal stress produced in the hybrid specimen during the manufacturing and effect of residual thermal stress on fracture toughness of interfaces, specimens have been designed to suit DCB ASTM D 5528. The main challenge in manufacturing of metal-composite hybrid specimen is significant difference in CTE of metal and composite parts. This mismatch of material's CTE is the main reason of thermal stress development during the manufacturing which could cause bending and distortion of whole specimen in the manufacturing phase. In addition, the residual thermal stress could alter the Energy Release Rate for the crack propagation and change the adhesive fracture behavior. Hence to avoid these problems, the design of hybrid specimen is based on controlling the thermal stress build-up during the manufacturing. To reach this objective, the design of hybrid specimens has been based on the following proposed guidelines.

1. Both arms of DCB hybrid specimen must have symmetric lay-ups, to avoid bending-extension coupling in each arm separated by interface layer

2. Equalization of overall CTE by same volumetric fraction of composite and titanium alloy in both arms, so to pretend of whole specimen bending

3. The bending modulus of the two arms must be the same in order to have symmetric response during DCB tests.

To investigate the objectives of this study, two specimens have been designed, Balanced and Un-Balanced. As it is indicated in Fig. 1, both type of specimens have the same materials and stacking sequence, but the position of pre-crack is different. Balanced specimen has been designed based on the proposed guideline. In the Balanced specimen, crack is located between two arms where each arm is symmetric independently from the other one with the same bending modulus and overall CTE, related to volumetric friction of material's percentage, is equalized, Fig.1-(a). In the Balanced specimen it

is expected that with the proposed design guideline thermal stress would be controlled.

To emphasize the effect of thermal stress built-up, Un-Balanced specimen has been designed. However, the Un-balanced specimen following the same lamination sequence and type of materials as balanced specimen, the position of pre-crack has been changed in the way that specimen did not have the conditions of semi-symmetric as proposed in the guideline, Fig.1.

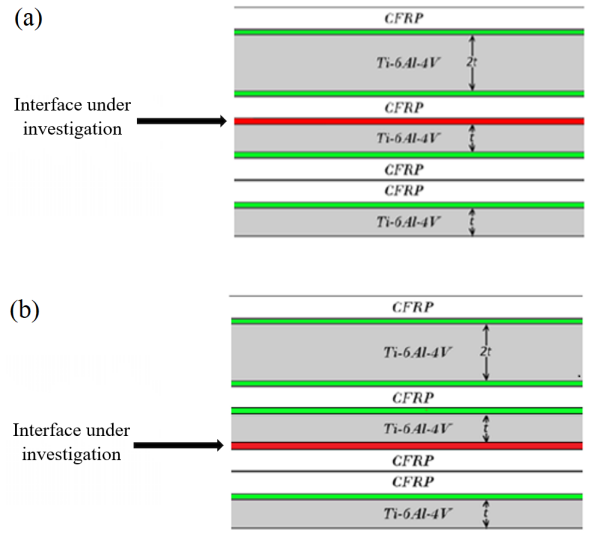

Figure 1: lamination sequence of hybrid laminates, (a) Balanced and (b) Un-Balanced specimen

Manufacturing of both Laminates had the same procedures despite of the pre-carck position. Laminates were produced with heat press plate apparatus, by using metallic mould and counter-mould and a soft frame made of silicon rubber as a dam. The composite-metal hybrid laminates have been produced by the technique of co-bonded which is more adequate for this type of structure as has been shown in previews study [13]. For this purpose, each interface of composite and metal part contains a layer of 3MTM Scotch-Weld AFK-163-2K adhesive. In addition, to increase the bonding of adhesive layer and metal sheet, titanium surfaces have been anodized. The artificial crack in the specimen has been produced by interposing double folded layer of Polytetrafluoroethylene (PTFE) with the length of 70 mm, in the interface of each laminate to obtain a pre-crack.

Metal-composite hybrid specimens are equipped by monitoring system contains of Optical Fiber (OF) carrying Fiber Bragg Gratings (FBG) sensors. This monitoring system is capable of capturing thermal stress build-up and its effect on fracture behavior by evaluating the strain evolution during manufacturing and fracture test. To fully assess the potential of optical fibre, two types of optical fibres are embedded inside each lamination. In the first type of fibres, the fibre core is protected by a polyacrylate coating, which is removed by chemical etching in correspondence of the position of 3 FBG sensors, positioned at distance of 27.5 mm. Coating removal, suggested by some authors [15], is aimed at providing an optimal transmission of strain experienced by the resin of composite material to the fibre core. The adopted fibres have a diameter of 250 μm , including coating, and of 125 μm without coating. In the second type of fibre, with a diameter of 195 μm, coating is made of a ceramic material (Ormocer®) and it is not removed from the fibre at sensors locations. Such fibres are endowed with two FBG sensors at distance of 50 mm. Additional optical fibre, which is embedded in the laminate between two adjacent specimens, are used to implement a direct measurement of temperature and allow a decoupling of mechanical and thermal contributions. This FBG sensor implanted loosely inside a steel capillary tube. So, the strain that experienced by the surrounding material cannot be transmitted to the isolated FBG sensor, which makes it sensitive only to temperature. The positions of sensors are illustrated in Fig. 2. The OFs were inserted by the distance of 2 plies close to the pre-cracked interface layer in composite parts of specimen.

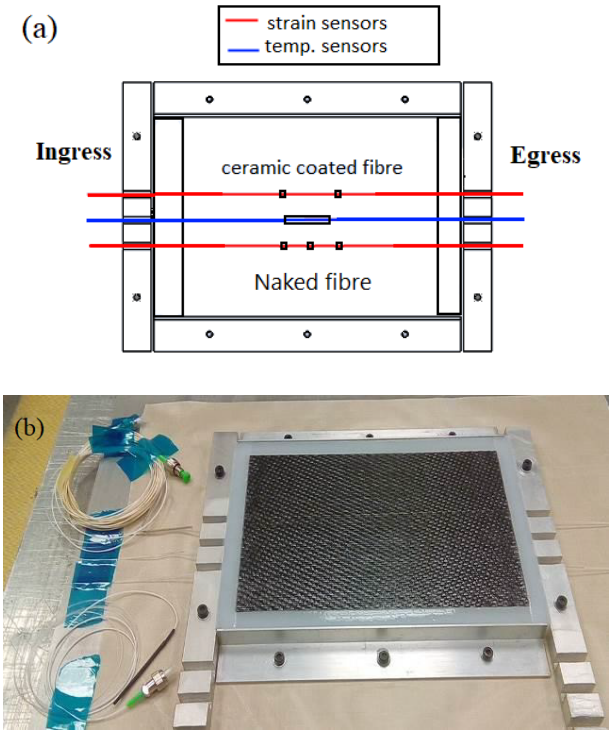

Figure 2: (a) Sensing network and position of FBGs in laminate, (b) lamination and embedment of fibers before curing

The sensing network containing of the Optical fibres carrying FBG sensors that has been embedded inside the laminations, Fig. 2-(a). Optical fibres were protected from possible damages at the egress and ingress of the laminate by using a PTFE tubing, which was partially embedded at the border of the laminate and passed through the silicon frame. The laminate had the dimension of 125 mm width and 200mm length. After manufacturing the narrow strip of laminate which was containing temperature sensor and 3 other specimens with the width of 25 mm and length of 200 mm have been cut from the laminate and prepared for DCB test.Two of them have been sensorized by Naked and Ormocer coated fibers and another is with-out sensor.

As described before one temperature sensor has been embedded in each laminate to capture the temperature cycles during the manufacturing phase. Fig. 3, illustrate the temperature cycles that has been reported by temperature FBG sensor based on time of production. The curing cycles was included of 3 steps: one hour at 100 °C, 2 hours at 180 °C, and final step which is Cooling to the 20 °C. The plot indicates that the internal temperature that has been captured by temperature sensor accurately followed the expected temperature cycles.

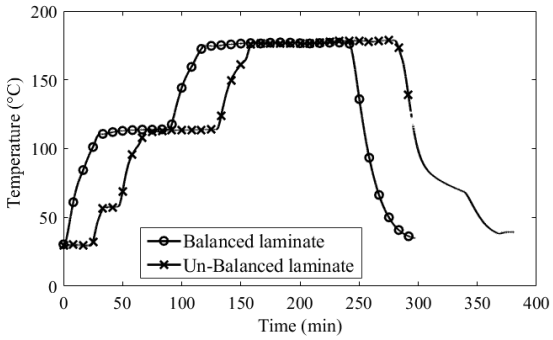

Figure 3: Temperature cycle of Balanced and Un-Balanced laminates captured by temperature FBG sensor

The strain that measured by FBG sensors, Naked and Ormocer-coated in Balanced and Un-Balanced laminations have been presented in Fig. 4. The wavelength has been shifted due to subtraction of temperature sensor's wavelength to capture pure mechanical respond of strain. As indicated in Fig. 4-(a), in the first minutes that pressure applied, Naked fibers and Ormocer-coated fibres had different response but at the end of the heating cycle the trends became similar. By neglection of initial offset, the measured strain from both Naked and Ormocer-coated fibres are similar. In Fig. 4-(b) which is presenting Un-Balanced specimen, FBG sensors indicating some oscillation in strain at beginning of curing cycle. This oscillation is because of removing the pressure at the begining of curing cycle to adjust the position of fibers.

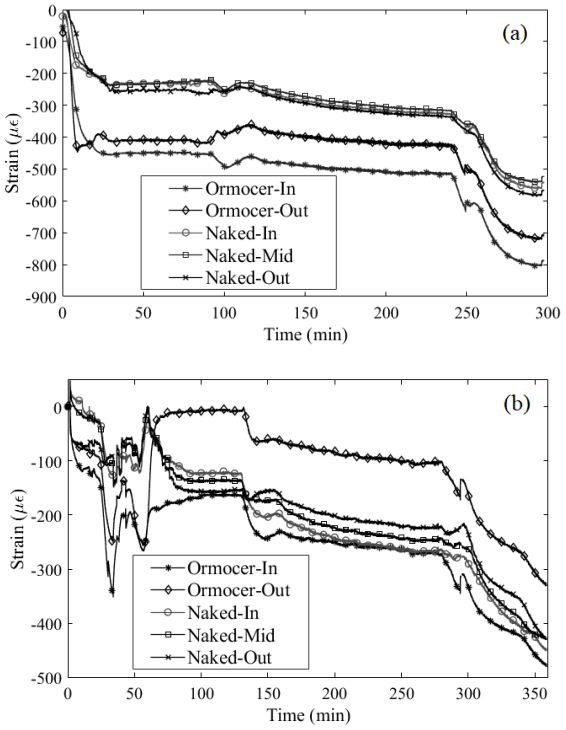

Figure 4: Strain evolution during the curing phase in (a) Balanced and (b) Un-Balanced specimen measured by FBG sensors

As has been expected from the numerical design of specimen, Balanced specimen had negligible spring back because of the equal overall bending stiffness in two arms but in the Un-Balanced specimen, lower arm which is also the weaker arm experienced some distortion after cooling, Fig.5.

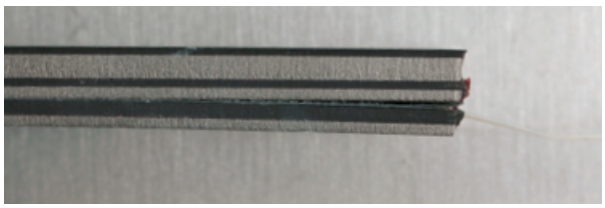

Figure 5: Spring back effect in Un-Balanced specimen after cooling

3. EXPERIMENTAL DCB TESTING

Three specimens from each lamination have been prepared for DCB test, two of them have been sensorized by Naked and Ormocer coated fibers, another one without sensors. These specimens have

been cut from the whole laminate by means of water jet cutter. According to ASTM D 5528 procedure, specimens have been conducted by pre-opening phase procedure. An MTS 858 hydraulic test system has been used for all the experiments. The force-displacement responses of Balanced and Un-Balanced specimens have been presented in Fig.6-(a) and (b). As indicated in the plots, the scattering of results in each type of specimen is quite limited and showing the same fracture behavior between all specimens of the same type.

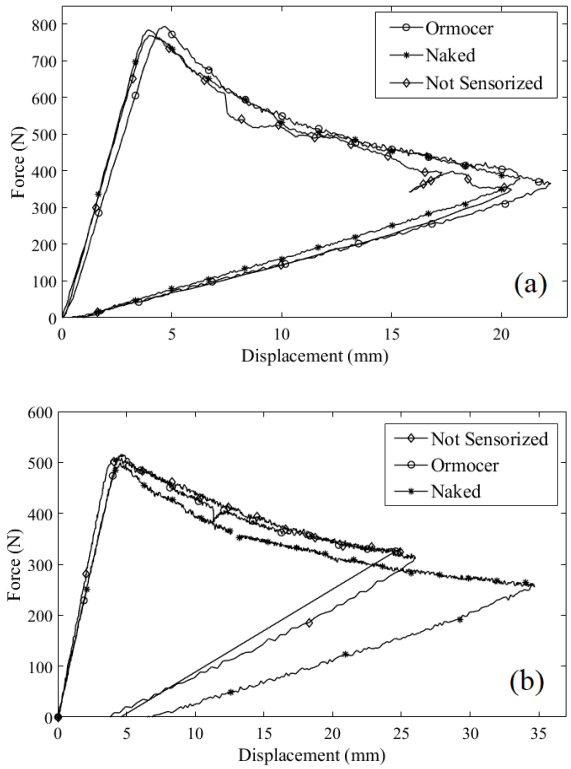

Figure 6: Force vs. Displacement of (a) Balanced and (b) Un-Balanced specimen

According to the results from balanced specimens, the very limited level of residual displacement was present at the end of the unloading phase, which does not exhibit bending distortion before and after crack opening. This is the confirmation for expected response of quasi-symmetric metal-composite laminates; however, in the Un-Balanced specimen which does not consider quasi-symmetric condition, the amount of residual displacement was higher. Crack propagation versus Displacement for both cases of Balanced and Un-Balanced presented in Fig.7-(a) and (b).

The Energy Release Rate (ERR) is evaluated for different crack lengths with the help of data reduction methods suggested by ASTM D 5528, Beam Theory (BT), Modified Beam Theory (MBT), Compliance Calibration (CC) and Modified Compliance Calibration (MCC). Fig.8 is presenting R-curves of Balanced specimens for both different sensorized specimens. Fracture toughness in mode I for Balanced specimen has limited scattering of data with average value of 3.3 (KJ/mm^2) from both kind of fiber coating.

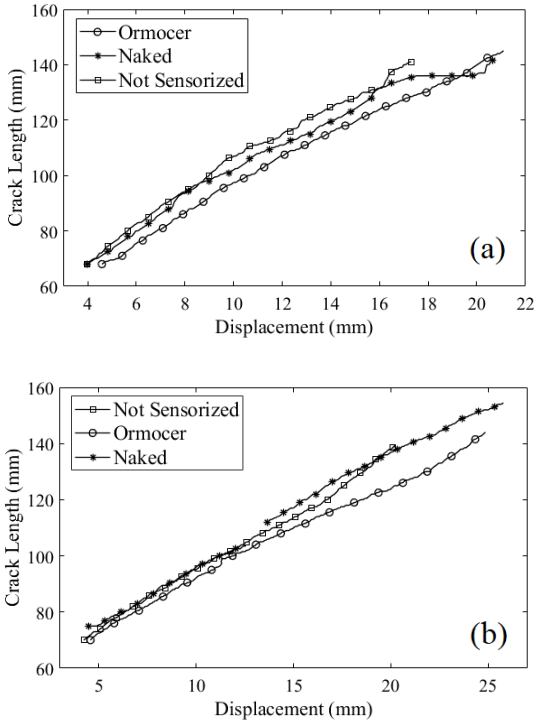

Figure 7: Crack propagation vs. Displacement of (a) Balanced and (b) Un-Balanced specimen

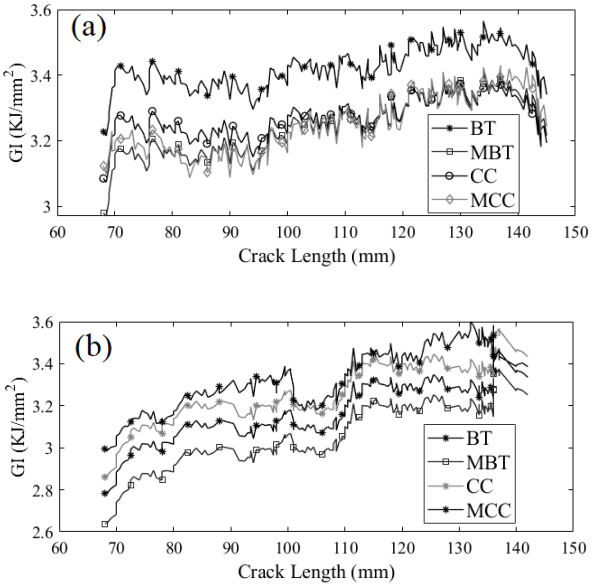

Figure 8: R-curves: (a) Ormocer fiber, (b) Naked fiber

4. NUMERICAL ANALYSIS OF DCB AND COOLING PHASE OF MANUFACTURING

4.1. Proposed cohesive modelling approach

Traditional cohesive zone modelling approach in explicit time integration scheme cause the high computational costs and numerical instability because of the direct effect of the very high penalty stiffness of the cohesive elements [18]. The new technique which is proposed by Airoldi et al. [19] based on In-plane and Out-of-plane stress components overcomes such difficulties.

By considering a laminate in a very simple bending condition, the roles of In-plane and Out-of-plane stress components can be pointed out, as in Fig.9.

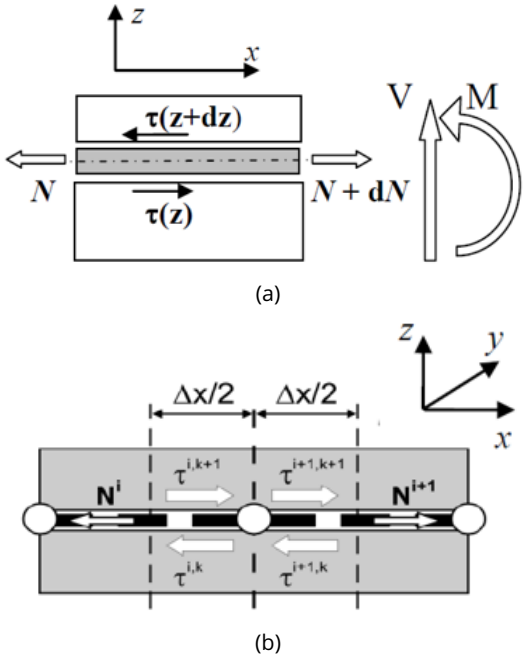

Figure 9: Stress resultants acting on a single lamina in bending conditions (a), and proposed finite element scheme (b)

As has been shown in Fig.9, the translational equilibrium can be formalized as Eq.(1), considering membrane force per unit width, N and shear stress transferred through the interface.

$$(1) \quad dN_{xx}/dx = \tau_{xz}(z+dz) - \tau_{xz}(z),$$

Conventional brick elements considered as interface elements because of capability of constitutive behavior of In-plane and Out-of-plane response. Relative displacements at the mid-planes could indicate the fracture process modes I, II and III, Fig.10. These three fracture modes are illustrated in Eq.3. By assumption of small displacement, Δ,

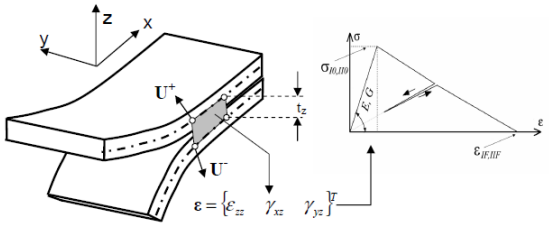

Figure 10: Fracture process described in the proposed modelling technique

strain state of solid element, ϵ can be written as Eq.2. If the vector of displacement discontinuities δ is conceptually replaced by Δ, Eq.3 can be used to convert a generic traction-displacement

$$(2) \quad \epsilon = \begin{bmatrix} \epsilon_{zz} & \gamma_{xz} & \gamma_{yz} \end{bmatrix}^T$$

$$(3) \quad \Delta_I = \begin{cases} \Delta_z & \text{if } \Delta_z > 0 \\ 0 & \text{if } \Delta_z \leq 0. \end{cases} ; \Delta_{II} = \Delta_{III} = \Delta_x$$

If the conventional traction-separation law is replaced by constitutive bi-linear response, such law is attributed to three-dimensional connection elements with null response in the in-plane stress components. Hence, the constitutive response attributed to the solid element will be Eq.4, where d is a scalar damage variable to represent the stiffness properties degradation during the evolution of the fracture process.

$$(4) \quad \begin{bmatrix} \sigma_{zz} \\ \tau_{xz} \\ \tau_{yz} \end{bmatrix} = \begin{bmatrix} E_{zz} & 0 & 0 \\ 0 & G_{xz} & 0 \\ 0 & 0 & G_{yz} \end{bmatrix} (1-d) \begin{bmatrix} \epsilon_{zz} \\ \gamma_{xz} \\ \gamma_{yz} \end{bmatrix}$$

The next step of this approach makes links between the critical energy release rates and the energy dissipated in the damage process. Eq.5 and Eq.6 presents the energy release rates for fracture modes I and II. In the constitutive model, properties in mode II and III are considered identical.

$$(5) \quad \int_0^\infty \sigma_{zz} d\Delta_I = t_k \int_0^\infty \sigma_{zz} d\epsilon_{zz} = G_{Ic}$$

$$(6) \quad \int_0^\infty \tau_{zz} d\Delta_{II} = t_k \int_0^\infty \tau_{zz} d\gamma_{zz} = G_{IIc}$$

According to this constitutive law, the components of Green-Lagrange strain tensor were used in Fortran Vumat Subroutine to link the cohesive law with the 3DS/Abaqus Explicit Code. This technique does not require traditional cohesive elements with zero thickness and non-physical penalty stiffness

which severely affect the computational costs and numerical performances. This method could be applied on 3D elements with physical consideration of stiffness for material characteristics.

4.2. Numerical simulation of cooling phase

The correct measurement of thermal stress build-up during the manufacturing is related to consideration of viscous response of polymeric materials, the effect of friction between laminate and apparatus and variability of CTE with temperature. The main purpose of this study is investigation on the effect of residual thermal stress on fracture behavior of interface between metal and composite part of hybrid specimen. To reach this objective, the remaining strain at the end of thermal analysis in numerical simulation must be equal to the amount of remaining strain that has been measured by FBG sensors inside the laminate. By plotting the strain versus the temperature in the cooling phase of the manufacturing process, it can be observed that for both lamination types, the trend of strain that have been captured by both kind of sensors are similar and non-linear; however, the sensors embedded in fiber direction, where CTE dependence of temperature should be relatively limited. This non-linearity could indicate the effect of friction between specimen and apparatus, because of total shrinkage of the specimen. In addition, the viscous behavior of the adhesive layers in interfaces of metallic parts and composite parts are another reason for the non-linear behavior of measured strain by FBG sensors.

As it is indicated in the Fig.11 and Fig.12 the strain during the cooling phase for both type of laminations from 180 °C to 110 °C is negligible but it starts to increase from110 °C to 20 °C. In addition, in the period of 180 °C to 110 °C, the effects of mentioned parameters which cause the non-linear behavior of strain are more significant.

To pursue the numerical modeling without the problems of non-linear behavior of strain, the thermal analysis of laminate just consider temperature in the period of 110 °C, to 20 °C, of cooling phase that strain has linear behavior. As they are illustrated in Fig.11 and Fig.12 the remaining strain at the end of simulation for both cases are similar to experimental results from FBG sensors. The numerical model is consisting of brick elements (C3D8R) for all the materials, even the layer of adhesive with the help of modeling technique that has been discussed above. The fracture behavior of interface layer is applied by the mean of Vumat as described before. To increase the accuracy of the modelling, the pressure that applied by heat press plate apparatus and friction between the specimen and the apparatus are also considered in analyses.

The Fig. 13 and Fig. 14 are indicating the stress produced in the Balanced and Un-Balanced specimens at the end of thermal analysis, respectively. However, as it has been expected, the Balanced specimen does not show significant amount of interlaminar stress, but in the Un-balanced specimen the amount of interlaminar stress is showing residual stress which can effect the fracture behavior in interface layer. As mentioned in the manufacturing section, Un-Balanced specimen had 1 mm distortion after cooling which is also captured by numerical modeling, Fig. 14.

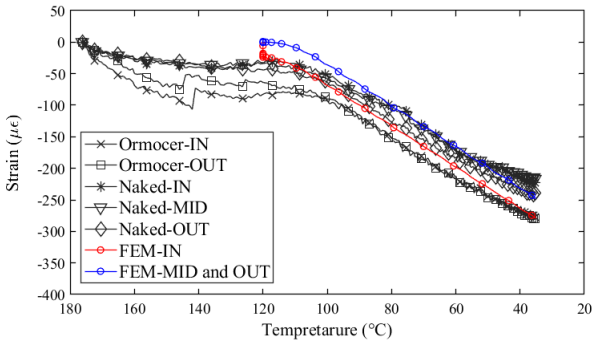

Figure 11: Strain evolution in cooling phase of Balanced specimen

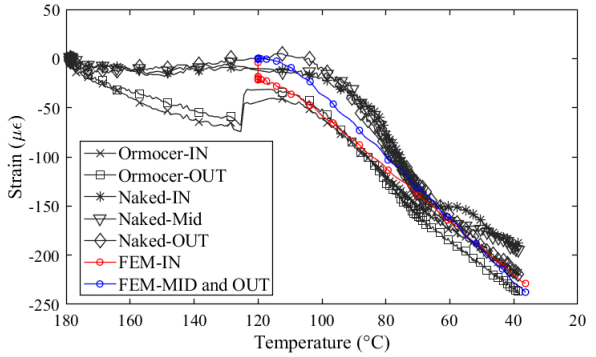

Figure 12: Strain evolution in cooling phase of Un-Balanced specimen

4.3. Experimental and Numerical Correlation in DCB fracture mechanic tests

The numerical Simulation of DCB loading is adopted on the same model of thermal analysis with the help of proposed cohesive modeling technique. Results of experimental test even with embedded FBG sensors does not show the amount of residual thermal stress and its effect on fracture behavior of adhesive layer. Hence, the overall experimental results

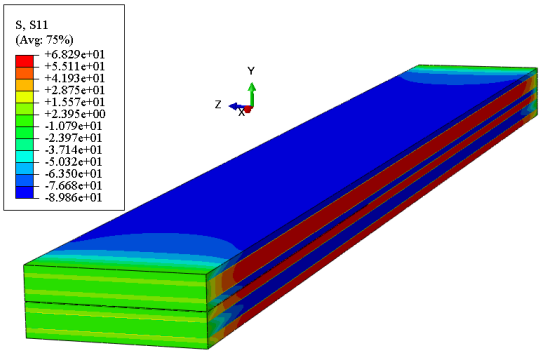

Figure 13: Strain evolution in cooling phase of Balanced specimen

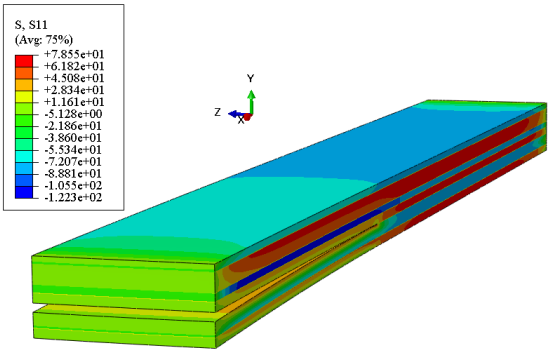

Figure 14: Strain evolution in cooling phase of Un-Balanced specimen

represent a significant benchmark for a numerical approach, in the scenes of numerical modeling validation.

The numerical modeling of DCB was developed by two types of loading conditions to indicate the effect of residual thermal stress in the fracture zone. In the first model, the analysis contains just simulating of DCB loading. In the second modeling, the analysis used the ability of ABAQUS in simulation of some steps subsequently. Hence, the effect of cooling has been implemented in the following steps. In the second modeling technique, after finishing of the cooling phase analysis, the pressure has been removed and analysis starts with DCB loading. In the Un-Balanced specimen after removing the pressure, high amplitude oscillation has been appeared in the DCB results which make the results unreadable. This oscillation caused by the energy trapped in the distorted lower arms which has been released after removing the pressure. The huge amount of this energy has been absorbed by a damper placed in the pressuring plate which has been just activate after finishing the first cooling analysis in the intermediate step between cooling and DCB to omit the oscillation from the results.

Fig. 15 presents the numerical-experimental correlation of force versus displacement for Balanced specimen in DCB loading. As it is expected, the Force-Displacement curve of Balanced specimen showing negligible effect of residual thermal stress; However, this effect is captured by assessment of strain during crack propagation, Fig. 16. as it is indicated in this plot, the numerical results with consideration of cooling is more close to experimental. The differences between Numerical results (with and without consideration of cooling) reveals the presents of thermal stress and its effect on strain evolution.

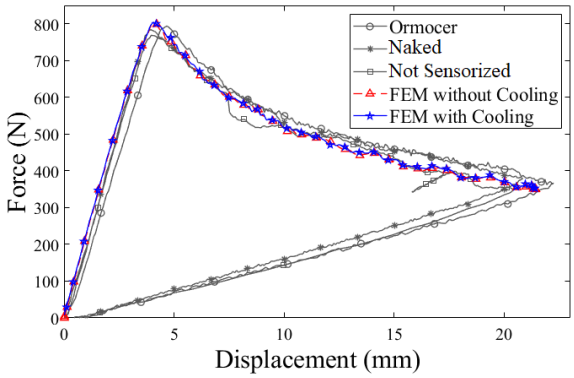

Figure 15: Comparison of Force vs Displacement for Numerical and experimental results in Balanced specimen

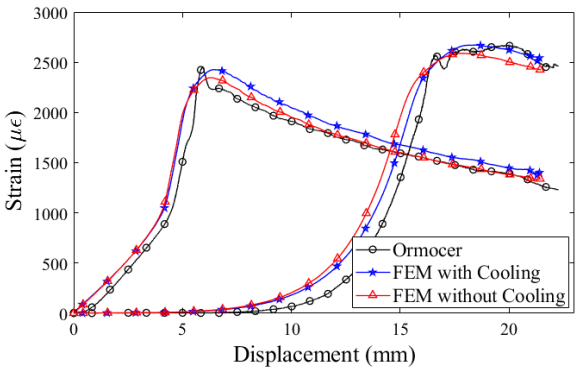

Figure 16: Strain evolution in DCB analysis of Balanced specimen

As mentioned before the Un-Balanced specimen has been designed to exaggerate the effect of thermal stress in the results. Fig. 18 presents the comparison of Force-Displacement for Numerical and experimental results. Contrarily of Balanced results, the effect of thermal stress is significant in fracture behaviour. As it is indicated in the experimental part of this study the adhesive material has been characterized by DCB test and ASTM D 5528 with Balanced specimen. Since All the numerical analysis using the

correct toughness of 3.3 (KJ/mm^2), it can be concluded that the adhesive layer has been degraded at the pre-crack tip. This effect has been omitted after 15 mm of crack propagation. This phenomena has been happened by the effect of distortion of lower arm. During the distortion, the lower arm has been curved (Fig.5) which caused the decrease in the thickness of adhesive layer and after omission of the effect of distortion, the material behave with the correct toughness.

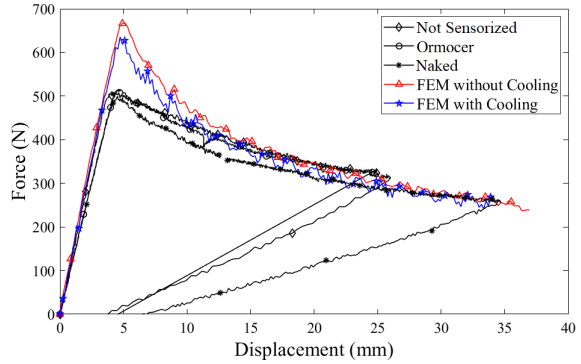

Figure 17: Comparison of Force vs Displacement for Numerical and experimental results in Un-Balanced specimen

The strain evolution versus displacement for naked fiber has been plotted in Fig. 18. The same as Balanced specimen, the effect of thermal stress is more significant in the plot of strain evolution. In this plot, the difference between numerical results of consideration of cooling and without cooling is more significant which has been expected from force-displacement results. From Fig. 18 it can be understood that the Numerical results with consideration of thermal residual stress has more accurate correlation with experimental results.

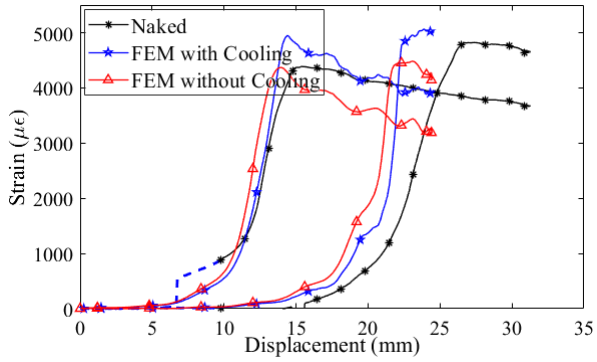

Figure 18: Comparison of Force vs Displacement for Numerical and experimental results in Un-Balanced specimen

5. CONCLUSION

In this paper a co-bonded titanium-unidirectional CFRP hybrid material has been investigated concentrating on the complex thermal residual strain and stresses generation during the manufacturing and the effect of this phenomena on the fracture behaviour in mode I. Monitoring of the manufacturing process by the means of FBG sensor provided significant information. With the help of capillary tube technique, the pure mechanical strain has been assessed during the manufacturing process. Indeed, all these sensors experienced initial offsets during the phase of mould closure and initial pressure application, but the behaviour in the subsequent phases of the process was different. However, it must be remarked that the slopes of the strain vs. temperature curves by all the FBG sensors of each lamination are very similar to each other.

In particular, the embedment of optical fibers close to interfaces has highlighted that the significant part of the residual strain and stress generation happens during the cooling process when solidification of the polymeric part of the specimen happened. By increasing the bonding between the layers during the cooling phase the load transmission capability at the interfaces has been enhanced.

Furthermore, the fracture process has been successfully monitored by FBG sensors. The correlation of Numerical and Experimental results reveals the effect of residual thermal stresses on the fracture behavior of specimen. Based on this results, such aspect is particularly relevant for application in the hot spots of structures, to easily detect structural damage that can develop during operations under conditions that can difficulty be accurately foreseen in the design phase. Such combination between the possibilities offered by optical fibre technology and the numerical prediction of sensing network performances is fundamental to design effective Usage and Health Monitoring System that could represent one of the most important features of future generation aircraft.

ACKNOWLEDGEMENT

The authors thanks Plyform composites s.r.l and Ing. Lorenzo Cartabia for the contribution in this work. This project has received funding from the European Union's H2020 research and innovation program under the Marie Skłodowska-Curie grant agreement No 721920.

REFERENCES

[1] Kessler, S., Spearing, S., and Soutis, C. (2002) Damage detection in composite materials using Lamb wave methods. *Smart Materials and Structures,* **11**(2), 269–278.

[2] Garcia, I., Zubia, J., Durana, G., Aldabaldetreku, G., Illarramendi, M., and Villatoro, J. (2015) Optical Fiber Sensors for Aircraft Structural Health Monitoring. *Sensors,* **15**(7), 497–519.

[3] Crane, R. M., Aleksander, R., Macander, B., and Gagorik, J. (1983) Fiber Optics for a Damage Assessment System for Fiber Reinforced Plastic Composite Structures. *Review of Progress in Quantitative Nondestructive Evaluation,* pp. 1419–1430.

[4] Dunphy, J. R., Meltz, G., Lamm, F. P., and Morey, W. W. (1990) Multifunction, distributed optical fiber sensor for composite cure and response monitoring. *Proceedings of Fiber Optic Smart Structures and Skins III, San Jose, USA,* (September).

[5] Kuang, K. S. C., Kenny, R., Whelan, M. P., Cantwell, W. J., and Chalker, P. R. (2001) Embedded fibre Bragg grating sensors in advanced composite materials. *Composites Science and Technology,* **61**(10), 1379–1387.

[6] Okabe, Y., Mizutani, T., Yashiro, S., and Takeda, N. (2002) Detection of microscopic damages in composite laminates with embedded small-diameter fiber Bragg grating sensors. *Composites Science and Technology,* **62**(7-8), 951–958.

[7] Giordano, M., Laudati, A., Nasser, J., Nicolais, L., Cusano, A., and Cutolo, A. (2004) Monitoring by a single fiber Bragg grating of the process induced chemo-physical transformations of a model thermoset. *Sensors and Actuators A: Physical,* **113**(2), 166–173.

[8] Wang, Y., Han, B., Bar-Cohen, A., and Cho, S. (2007) Fiber Bragg Grating Sensor to Characterize Curing Process-dependent Mechanical Properties of Polymeric Materials. *Proceedings of Electronic Components and Technology Conference 57th,*.

[9] Chiang, C.-C. and Tesinova, P. (2011) Curing monitoring of composite material using embedded fiber Bragg grating sensors. *Advances in Composite Materials - Analysis of Natural and Man-Made Materials,* pp. 345–360.

[10] Wisnom, M., Gigliotti, M., Ersoy, N., Campbell, M., and Potter, K. (2006) Mechanisms generating residual stress and distortion during manufacturing of polymer matrix composite structures. *Composites Part A: Applied Science and Manufacturing,* **37**(4), 522–529.

[11] Parleviet, P., Bersee, H., and Beukers, A. (2006) Residual stresses in thermoplastic composites - a study of literature - part I: formation of resisual stresses. *Composites Part A: Applied Science and Manufacturing,* **37**(11), 1847–1857.

[12] Zobeiry, N. and Poursatib, A. (2015) The origin of residual stress and its evaluation in composite materials. *Structural Integrity and Durability of Advanced Composites: Innovative Modelling Methods and Intelligent Design,* pp. 43–72.

[13] Airoldi, A., Bettini, P., Fournier, S., Capizzi, G., and Stella, M. nad Bogotto, P. (2017) Modelling and monitoring the response of bonded composite/metallic structures during manufacturing process and damage evolution. *NATO Science and Technology Organization, Turin, Italy,*.

[14] Baldi, A., Airoldi, A., Crespi, M., Iavarone, P., and Bettini, P. (2011) Modelling competitive delamination and debonding phenomena in composite t-joints. *Proced Eng,* **10**, 3483–3489.

[15] Sorensen, L., Gmur, T., and Botsis, J. (September, 2004) Residual strain development in lamianted thermoplastic composites measured using fibre Bragg grating sensors. *Proceedings of CompTest 2004 conference, Bristol, UK,* pp. 145–146.

[16] Parleviet, P., Bersee, H., and Beukers, A. (2007) Residual stresses in thermoplastic composites - a study of literature - part II: experimental techniques. *Composites Part A: Applied Science and Manufacturing,* **38**(3), 651–665.

[17] Sala, G., Di Landro, L., Airoldi, A., and Bettini, P. (2015) Fibre optic health monitoring for aeronauical applications. *Meccanica,* **50**(10), 2547–2567.

[18] Abaqus 6.11 Documentation., Providence (RI, USA): Dass ault Systemes Simulia Corp.

[19] Airoldi, A., Sala, G., Bettini, P., and Baldi, A. (2013) An efficient approach for modeling interlaminar damage in composite laminates with explicit FE codes. *Journal of Reinforced Plastics and Composites,* **32**(15), 1075–1091.